Measurements of Transverse Spin Dependent $\pi^+\pi^-$ Azimuthal Correlation Asymmetry and Unpolarized $\pi^+\pi^-$ Cross Section in *pp* Collisions at $\sqrt{s}$ = 200 GeV at STAR

Babu Pokhrel
(For the STAR Collaboration)
03/30/2023

Supported in part by:
U.S. DEPARTMENT OF ENERGY | Office of Science

Motivation

Proton Structure

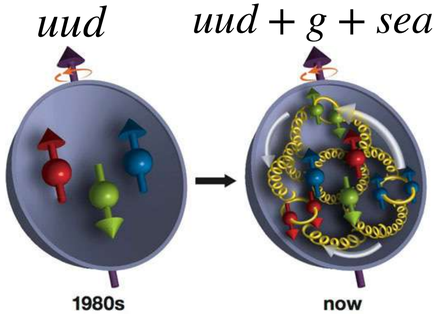

- Proton structure studied in terms of parton distribution functions (PDFs).
- Leading order PDFs:

Unpolarized: $f(x) \approx$

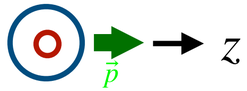

Helicity: $g(x) \approx$

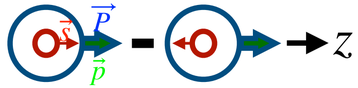

Transversity: $h_1(x) \approx$

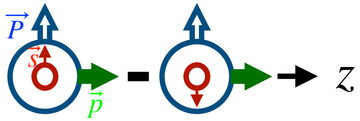

$\vec{P}$ = Nucleon polarization

$\vec{p}$ = Nucleon momentum

$\vec{s}$ = Quark polarization

z = Proton's momentum axis

Motivation

Proton Structure

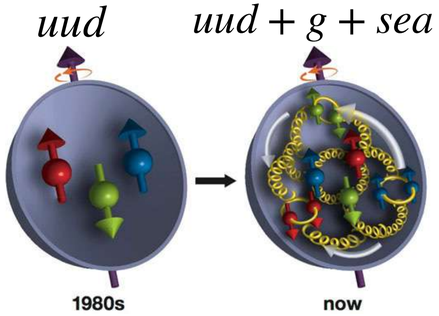

- Proton structure studied in terms of parton distribution functions (PDFs).
- Leading order PDFs:

Unpolarized: $f(x) \approx$ 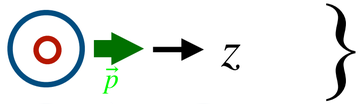

Helicity: $g(x) \approx$ 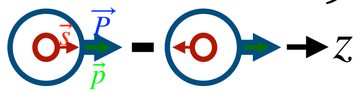

Transversity: $h_1(x) \approx$ 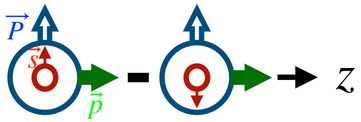

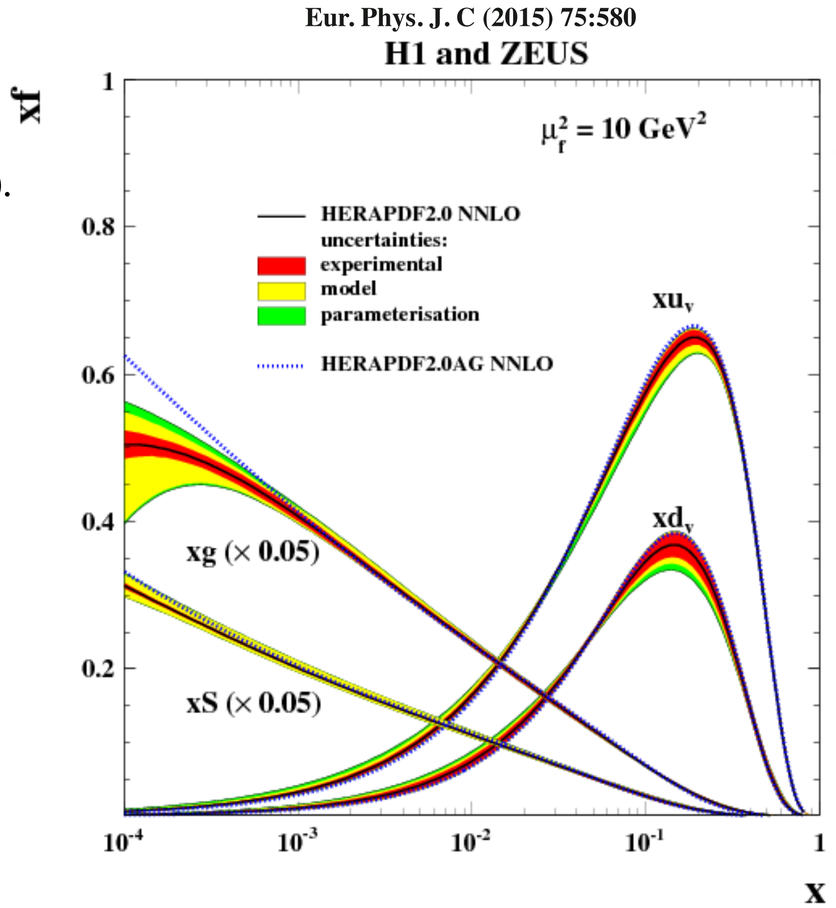

- Well constrained by the SIDIS data.

$\vec{P}$ = Nucleon polarization

$\vec{p}$ = Nucleon momentum

$\vec{s}$ = Quark polarization

z = Proton's momentum axis

Motivation

Proton Structure

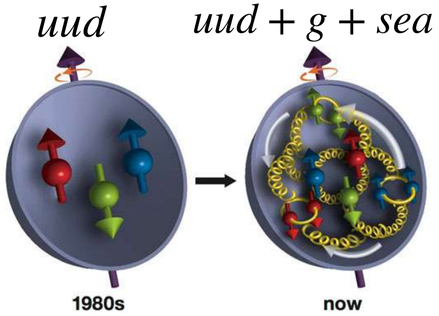

- Proton structure studied in terms of parton distribution functions (PDFs).
- Leading order PDFs:

Unpolarized: $f(x) \approx$ 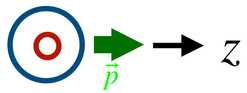

Helicity: $g(x) \approx$ 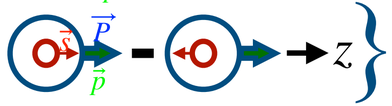

Transversity: $h_1(x) \approx$ 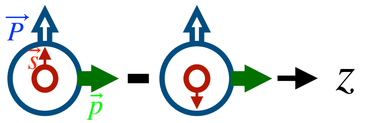

- Evidence of non-zero gluon polarization from the STAR data.

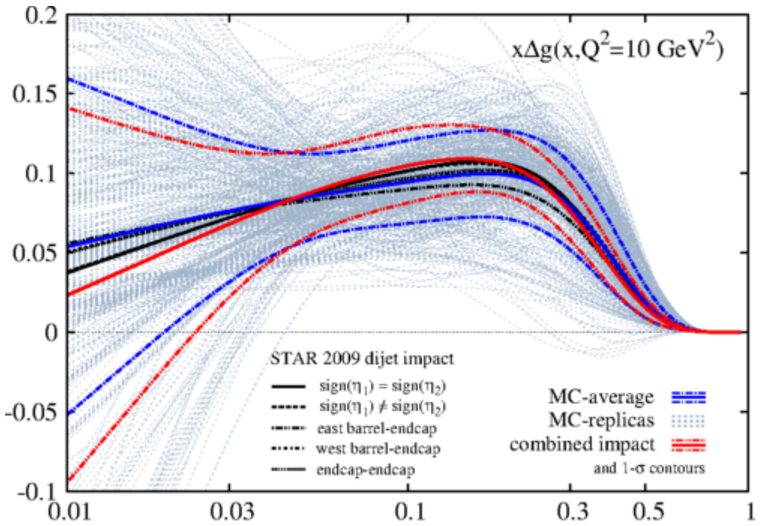

Daniel de Florian et. al. Phys. Rev. D 100, 114027 (2019)

NNPDF, Nucl. Phys. B887(2014)276-308

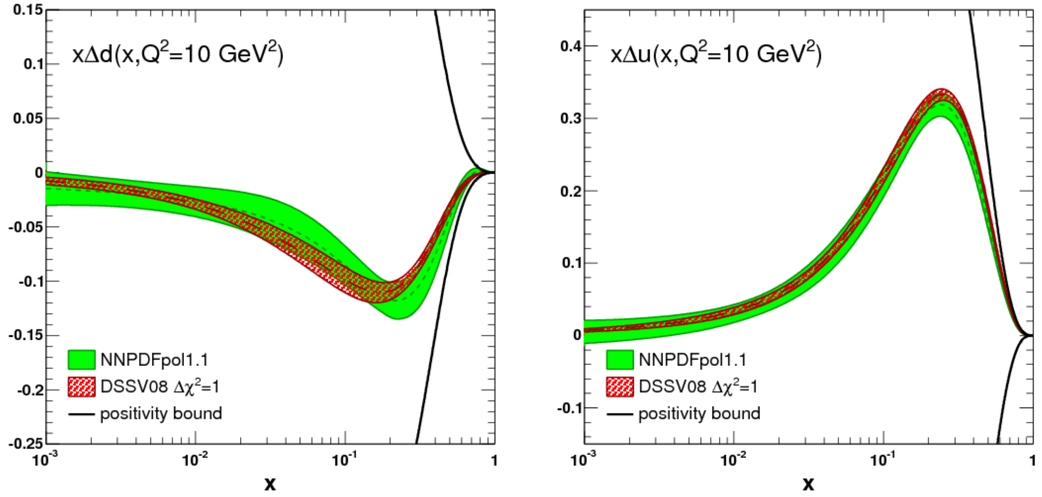

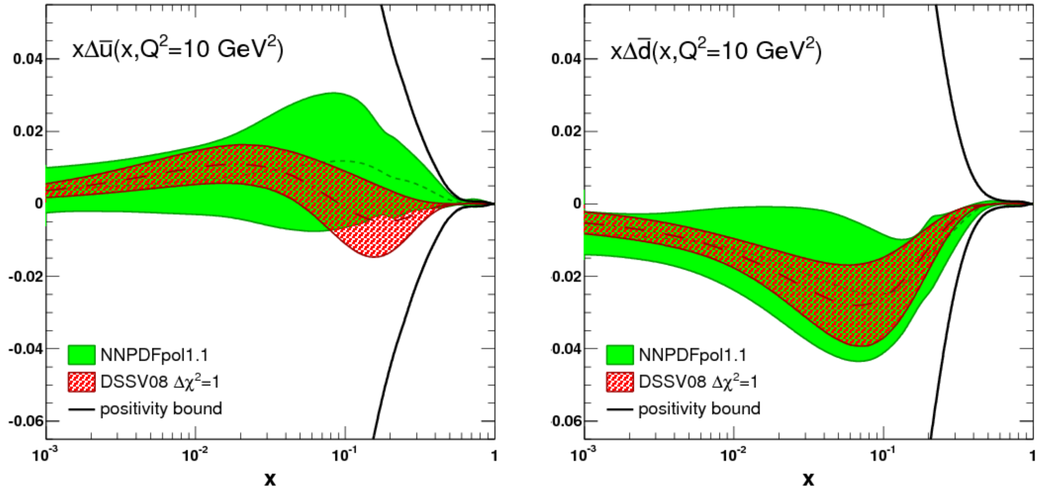

$\vec{P}$ = Nucleon polarization

$\vec{p}$ = Nucleon momentum

$\vec{s}$ = Quark polarization

z = Proton's momentum axis

Motivation

Proton Structure

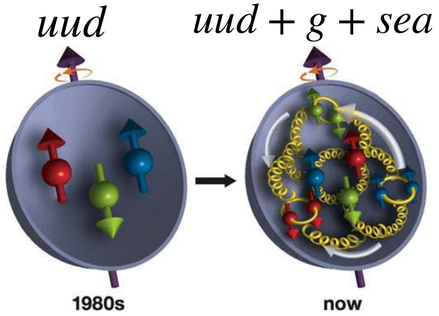

- Proton structure studied in terms of parton distribution functions (PDFs).
- Leading order PDFs:

Unpolarized: $f(x) \approx$ 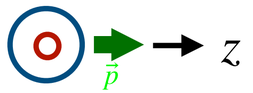

Helicity: $g(x) \approx$ 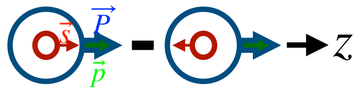

Transversity: $h_1(x) \approx$ 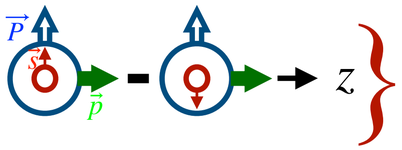

- $h_1(x)$ is least known, as it is not easily accessible in the physical process.
- $h_1(x)$ has gained a lot of attention lately, as it provides access to the **nucleon tensor charge** - an important nucleon property.

$\vec{P}$ = Nucleon polarization

$\vec{p}$ = Nucleon momentum

$\vec{s}$ = Quark polarization

z = Proton's momentum axis

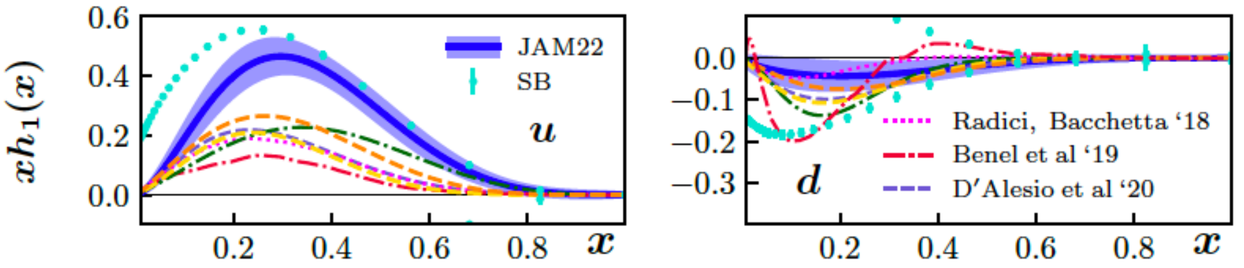

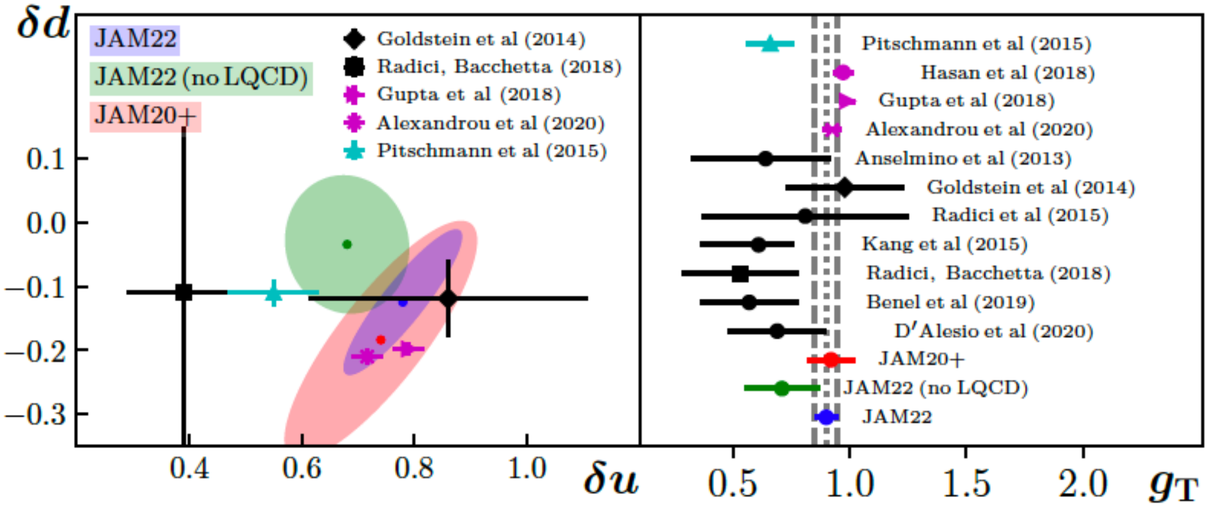

JAM Collab., Phys.Rev.D 106 (2022) 3, 034014

Motivation

Transversity ($h_1^q(x)$)

- Helicity flipped amplitude.
- Chiral-odd; conservation of chirality requires another chiral-odd counterpart to be appeared in the physical process.
- Measurement is not possible in inclusive DIS.

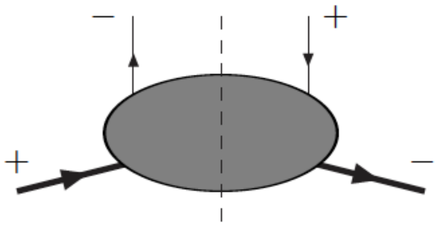

Motivation

Transversity ($h_1^q(x)$)

- Helicity flipped amplitude.
- Chiral-odd; conservation of chirality requires another chiral-odd counterpart to be appeared in the physical process.
- Measurement is not possible in inclusive DIS.

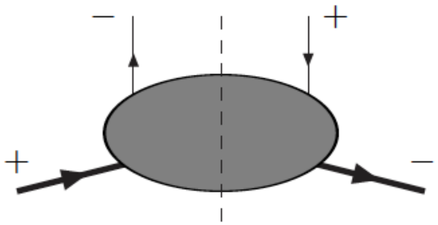

Proton-proton (pp) collisions provide multiple opportunities for the $h_1^q(x)$ measurement.

• Identified hadron inside jet (Collins Channel)

$p^{\uparrow} + p \rightarrow jet + h + X \sim h_1^q(x) H_1^{\perp}(z, j_T)$

- $h_1^q(x)$ coupled with the Collins FF, $H_1^{\perp}$.
- j_T = pion momentum transverse to the jet axis.
- $z = p_\pi / p_{jet}$

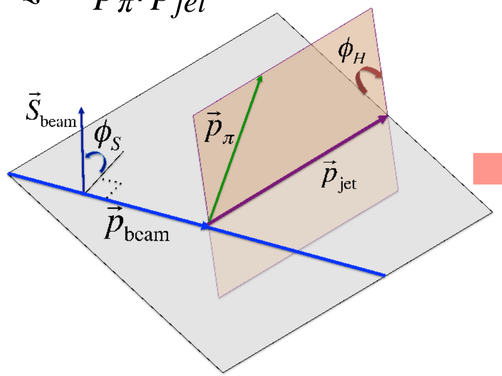

• Exclusively produced dihadron (Dihadron Channel)

$p^{\uparrow} + p \rightarrow h^+h^- + X \sim h_1^q(x) H_1^{\sphericalangle}(z, M)$

- $h_1^q(x)$ coupled with the interference FF (IFF), $H_1^{\sphericalangle}$.
- $z = \mathrm{E}^{\mathrm{h^+h^-}}/\mathrm{E}^{\mathrm{quark}}$, M = h^+h^- invariant mass

Observed azimuthal asymmetry due to the quark transverse polarization:

$A_{UT}^{\sin(\phi_S - \phi_H)} \sim h_1^q(x) H_1^{\perp}(z, j_T)$

$A_{UT}^{\sin(\phi_S - \phi_R)} \sim h_1^q(x) H_1^{\sphericalangle}(z, M)$

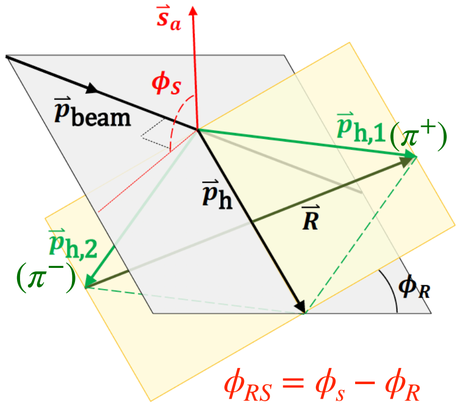

- Identified hadron-in-jet
- TMD formalism

- No jet reconstruction required
- Collinear approach

Observables for $h_1^q(x)$ *via* Dihadron Channel in *pp*

Reaction Channel: $p^{\uparrow} + p \rightarrow \pi^+\pi^- + X$

$\vec{p}_h = \vec{p}_{h,1} + \vec{p}_{h,2}$, $\vec{R} = \frac{1}{2}(\vec{p}_{h,1} - \vec{p}_{h,2})$, Spin transfer *via* $\sim \vec{s}_a \cdot (\vec{R} \times \vec{p}_h)$

Quark polarization favors $\pi^+\pi^-$ production to one direction in azimuth (ϕ_{RS}) resulting in azimuthal correlation asymmetry, $A_{UT}^{sin(\phi_{RS})}$.

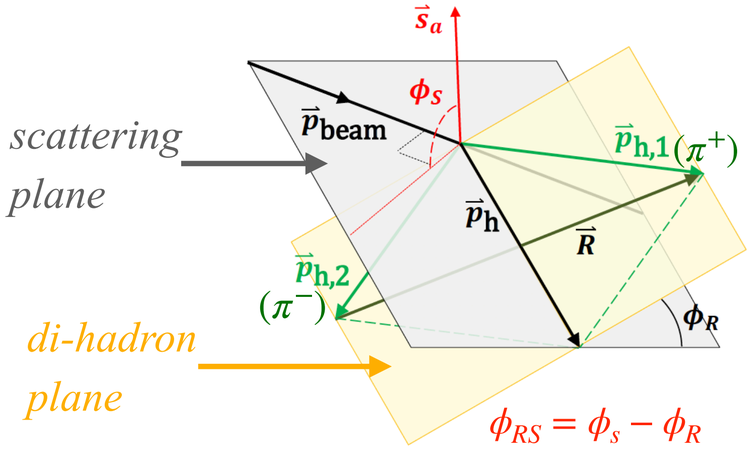

Observables for $h_1^q(x)$ *via* Dihadron Channel in *pp*

Reaction Channel: $p^{\uparrow} + p \rightarrow \pi^+\pi^- + X$

$\vec{p}_h = \vec{p}_{h,1} + \vec{p}_{h,2}$, $\vec{R} = \frac{1}{2}(\vec{p}_{h,1} - \vec{p}_{h,2})$, Spin transfer *via* $\sim \vec{s}_a \cdot (\vec{R} \times \vec{p}_h)$

Quark polarization favors $\pi^+\pi^-$ production to one direction in azimuth (ϕ_{RS}) resulting in azimuthal correlation asymmetry, $A_{UT}^{\sin(\phi_{RS})}$.

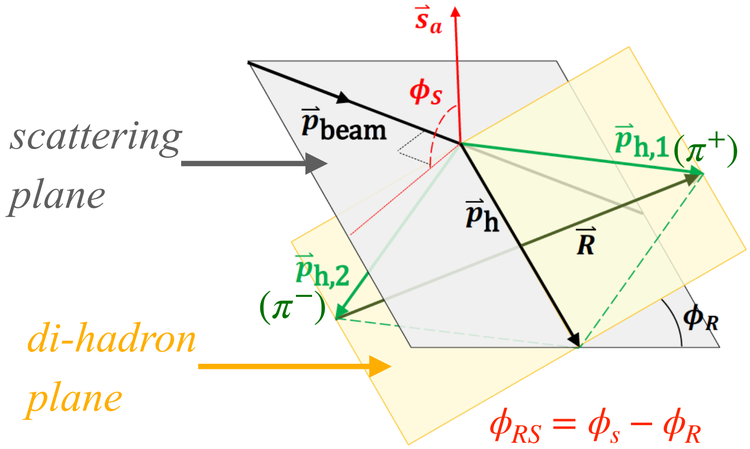

$\pi^+\pi^-$ Correlation Asymmetry:

$$A_{UT}^{\sin(\phi_{RS})} = \frac{d\sigma^{\uparrow} - d\sigma^{\downarrow}}{d\sigma^{\uparrow} + d\sigma^{\downarrow}} \propto \frac{\sum_{i,j,k} h_1^{i/p_a}(x_a) f_1^{j/p_b}(x_b) H_1^{\sphericalangle h_1 h_2/k}(z, M_h)}{\sum_{i,j,k} f_1^{i/p_a}(x_a) f_1^{j/p_b}(x_b) D_1^{h_1 h_2/k}(z, M_h)}$$

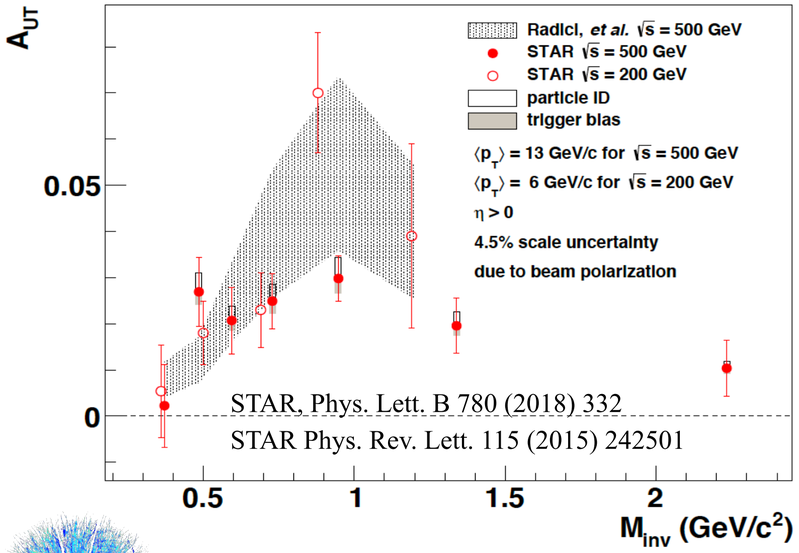

- $A_{UT}^{\sin(\phi_{RS})}$ is sensitive to the product $h_1(x)H_1^{\sphericalangle}(z, M)$.
- STAR observed significant $A_{UT}^{\sin(\phi_{RS})}$ signal, enhanced around the $\rho-$mass ($M_{inv} \sim 0.8$ GeV/c²) - expected due to the interference of hadrons produced via different channel.

Observables for $h_1^q(x)$ *via* Dihadron Channel in *pp*

Reaction Channel: $p^{\uparrow} + p \rightarrow \pi^+\pi^- + X$

$\vec{p}_h = \vec{p}_{h,1} + \vec{p}_{h,2}$, $\vec{R} = \frac{1}{2}(\vec{p}_{h,1} - \vec{p}_{h,2})$, Spin transfer *via* $\sim \vec{s}_a \cdot (\vec{R} \times \vec{p}_h)$

Quark polarization favors $\pi^+\pi^-$ production to one direction in azimuth (ϕ_{RS}) resulting in azimuthal correlation asymmetry, $A_{UT}^{sin(\phi_{RS})}$.

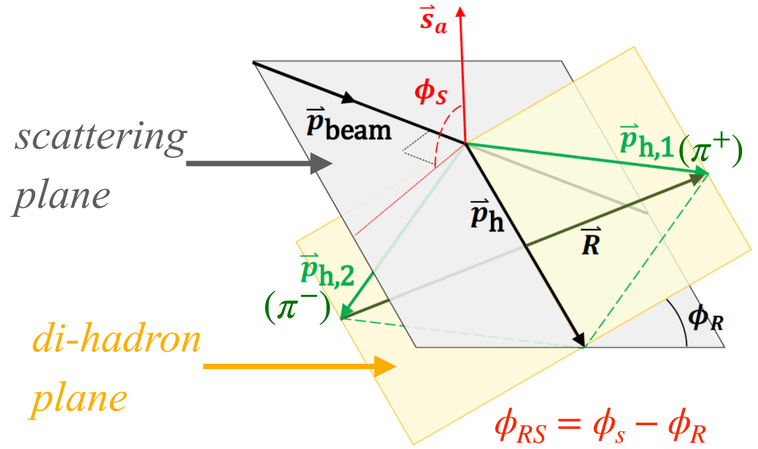

$\pi^+\pi^-$ Correlation Asymmetry:

$$A_{UT}^{sin(\phi_{RS})} = \frac{d\sigma^{\uparrow} - d\sigma^{\downarrow}}{d\sigma^{\uparrow} + d\sigma^{\downarrow}} \propto \frac{\sum_{i,j,k} h_1^{i/p_a}(x_a) f_1^{j/p_b}(x_b) H_1^{\sphericalangle h_1 h_2/k}(z, M_h)}{\sum_{i,j,k} f_1^{i/p_a}(x_a) f_1^{j/p_b}(x_b) D_1^{h_1 h_2/k}(z, M_h)}$$

- spin averaged FF, D_1.
- dominant uncertainty in $h_1^q(x)$, specifically from D_1 for gluon.
- **Unpolarized $\pi^+\pi^-$ cross section, $\sigma^{\pi^+\pi^-}$, give access to $D_1^{\pi^+\pi^-}$ in *pp*.**

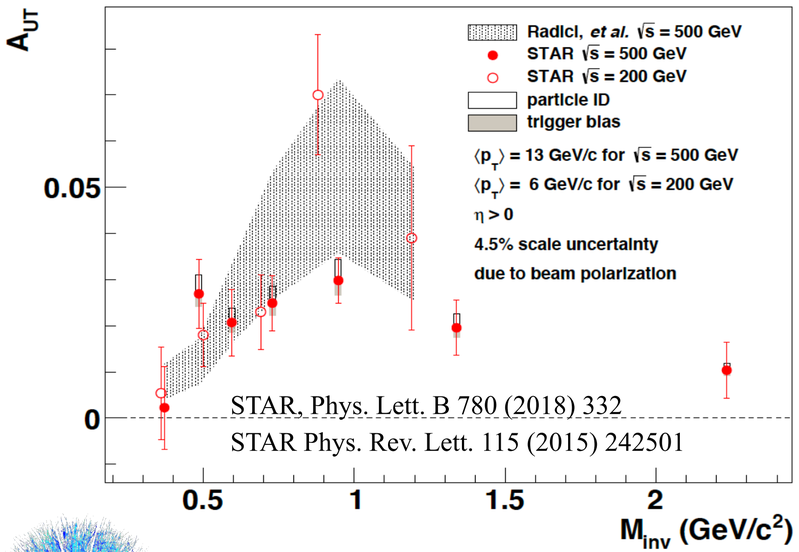

- $A_{UT}^{sin(\phi_{RS})}$ is sensitive to the product $h_1(x)H_1^{\sphericalangle}(z, M)$.
- STAR observed significant $A_{UT}^{sin(\phi_{RS})}$ signal, enhanced around the $\rho-$mass ($M_{inv} \sim 0.8$ GeV/c²) - expected due to the interference of hadrons produced via different channel.
- **Significant impact on the $h_1(x)$ from STAR data at 200 GeV in the valence region ($0.1 < x < 0.3$).**

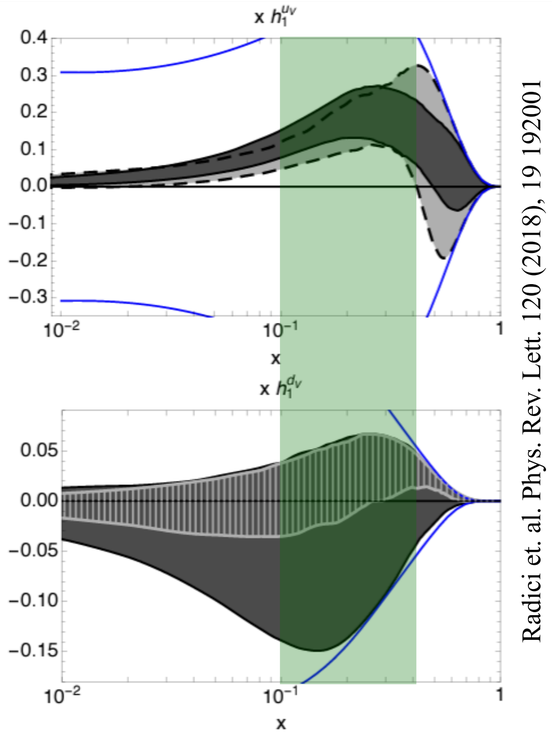

Relativistic Heavy Ion Collider (RHIC)

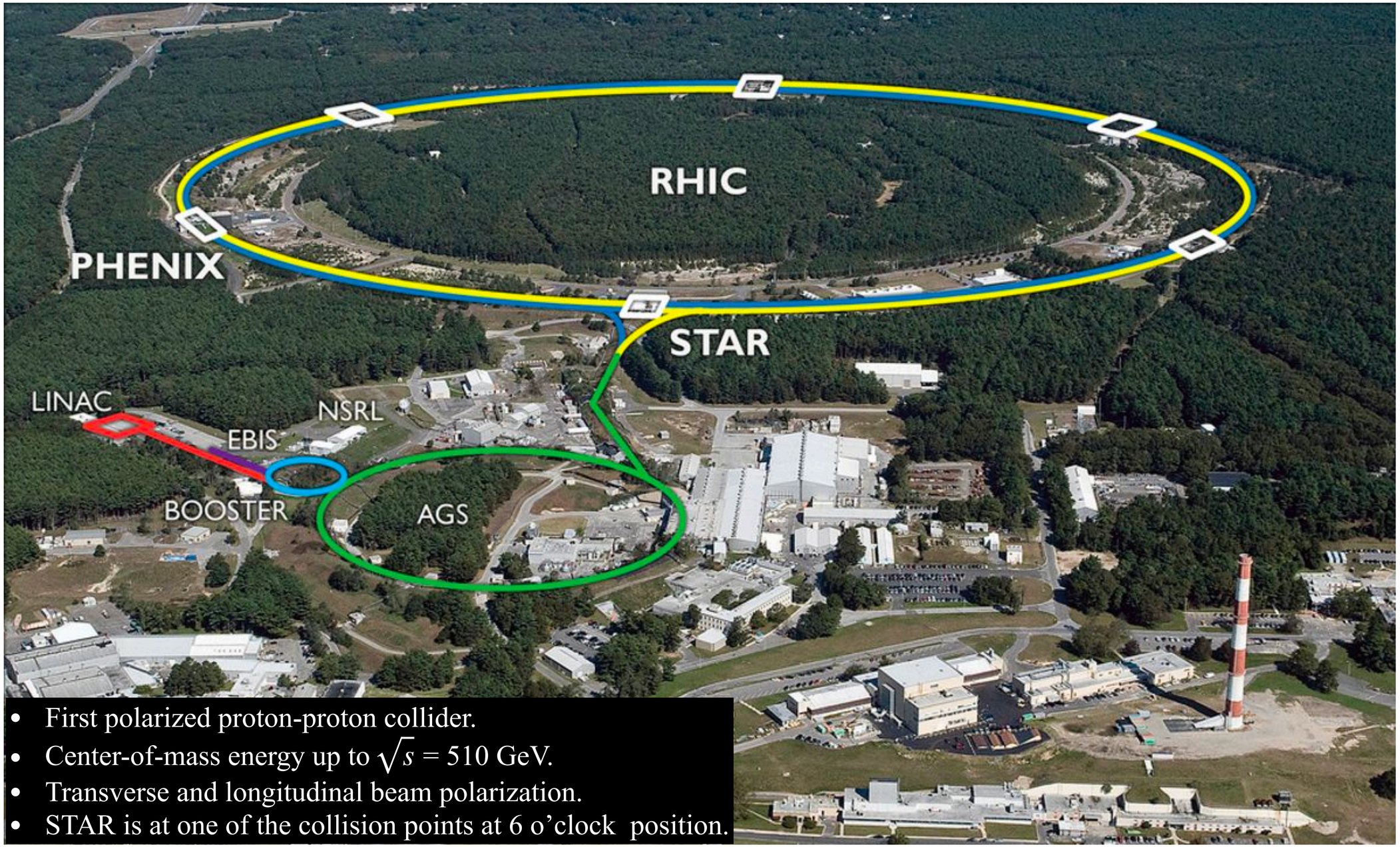

- First polarized proton-proton collider.
- Center-of-mass energy up to $\sqrt{s}$ = 510 GeV.
- Transverse and longitudinal beam polarization.
- STAR is at one of the collision points at 6 o'clock position.

Relativistic Heavy Ion Collider (RHIC)

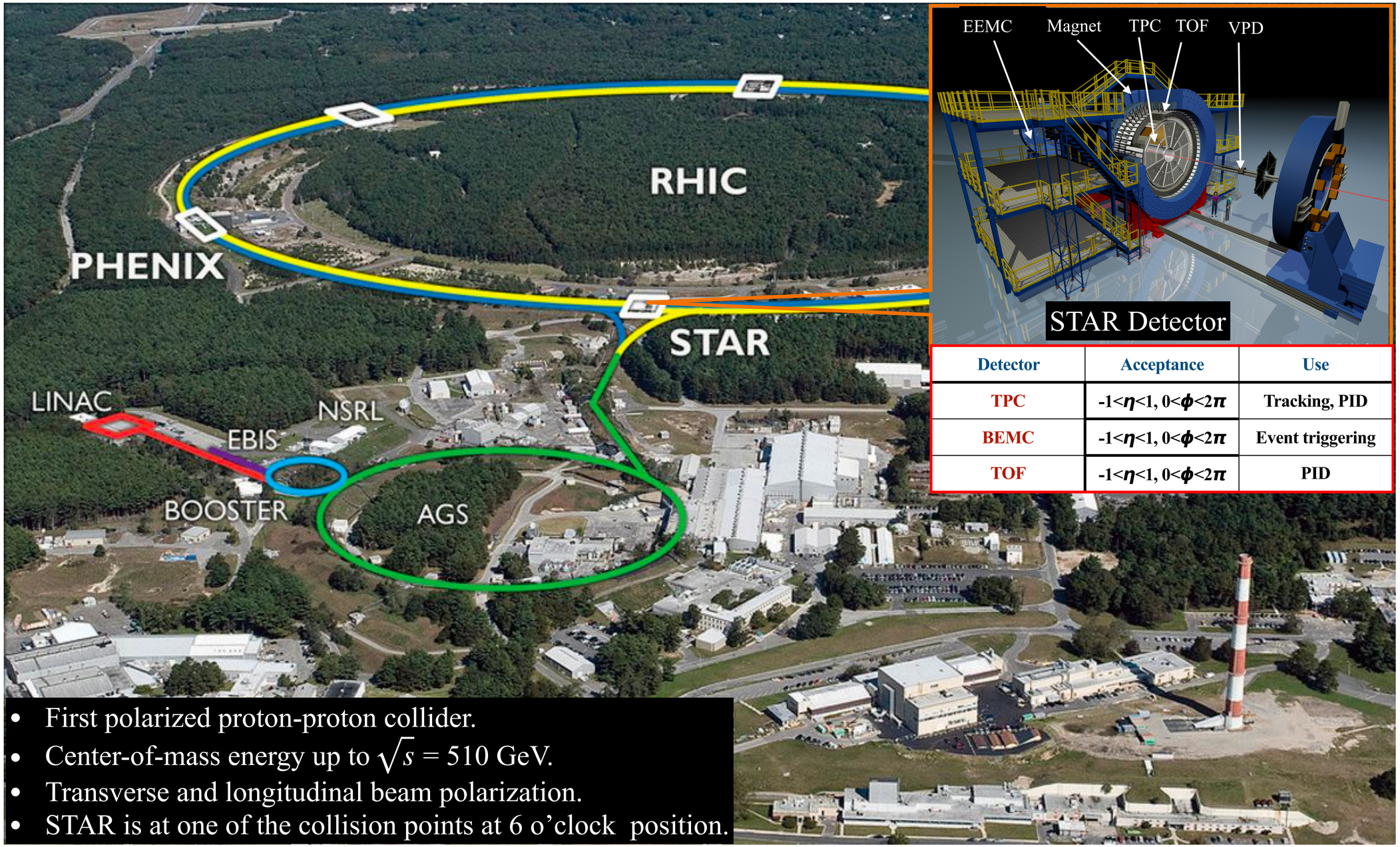

Detector	Acceptance	Use
TPC	$-1<\eta<1$, $0<\phi<2\pi$	Tracking, PID
BEMC	$-1<\eta<1$, $0<\phi<2\pi$	Event triggering
TOF	$-1<\eta<1$, $0<\phi<2\pi$	PID

- First polarized proton-proton collider.
- Center-of-mass energy up to $\sqrt{s}$ = 510 GeV.
- Transverse and longitudinal beam polarization.
- STAR is at one of the collision points at 6 o'clock position.

Relativistic Heavy Ion Collider (RHIC)

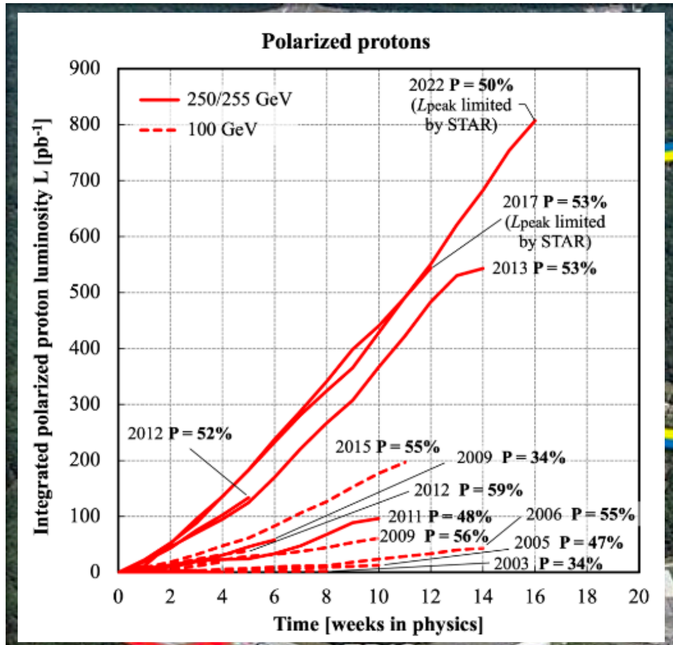

Detector	Acceptance	Use
TPC	$-1<\eta<1$, $0<\phi<2\pi$	Tracking, PID
BEMC	$-1<\eta<1$, $0<\phi<2\pi$	Event triggering
TOF	$-1<\eta<1$, $0<\phi<2\pi$	PID

- First polarized proton-proton collider.
- Center-of-mass energy up to $\sqrt{s}$ = 510 GeV.
- Transverse and longitudinal beam polarization.
- STAR is at one of the collision points at 6 o'clock position.

Relativistic Heavy Ion Collider (RHIC)

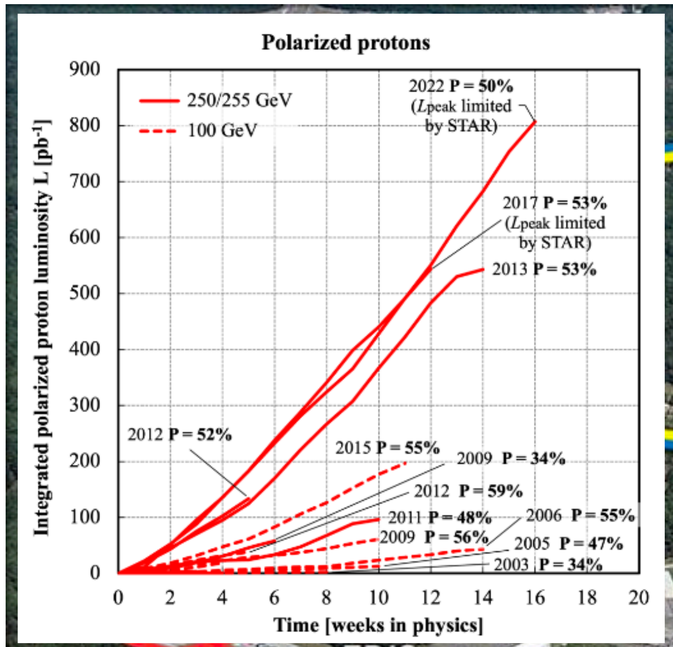

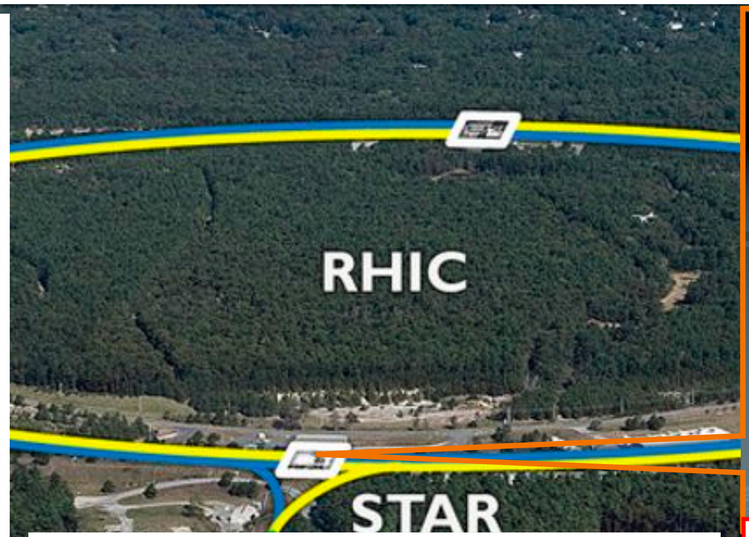

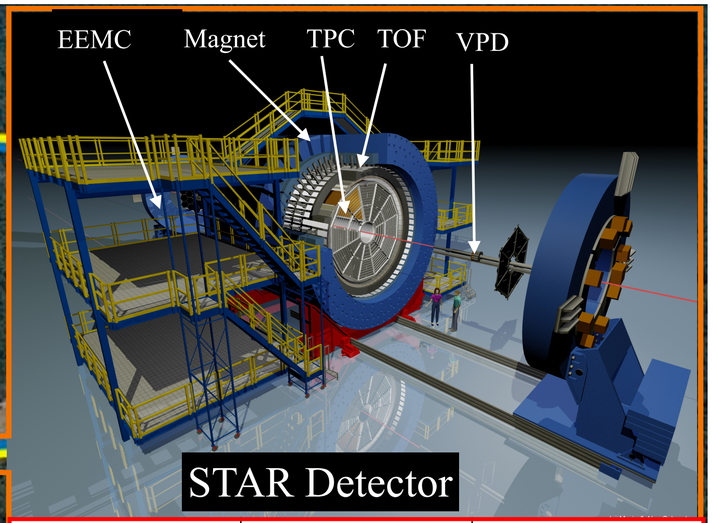

Detector	Acceptance	Use
TPC	$-1<\eta<1$, $0<\phi<2\pi$	Tracking, PID
BEMC	$-1<\eta<1$, $0<\phi<2\pi$	Event triggering
TOF	$-1<\eta<1$, $0<\phi<2\pi$	PID

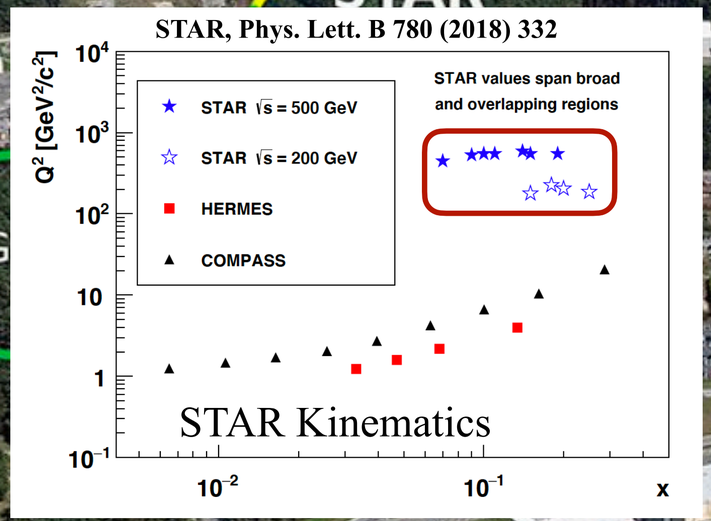

- First polarized proton-proton collider.
- Center-of-mass energy up to $\sqrt{s}$ = 510 GeV.
- Transverse and longitudinal beam polarization.
- STAR is at one of the collision points at 6 o'clock position.

STAR Run 2015 Precision $A_{UT}^{\sin(\phi_{RS})}$ Measurement

- **Event Selection**
  - This dataset provides the most precise A_{UT} at $\sqrt{s} = 200$ GeV to date.
  - Triggers : JP1, JP2
  - Pion selection: $|\eta| < 1,\ 1.5 < p_T < 15$ GeV/c, $-1 < n\sigma_\pi < 2$
  - All possible pion pairs of opposite charge.
  - Fix charge ordering in a pair: $\vec{p}_{h,1} = \pi^+$, $\vec{p}_{h,2} = \pi^-$
  - $\pi^+\pi^-$ selection cuts:

    cone < 0.7, $|\eta^{\pi^+\pi^-}| < 1$, $1 < p_T^{\pi^+\pi^-} < 15$ GeV/c, $0.27 < M_{inv} < 4$ GeV/c^2

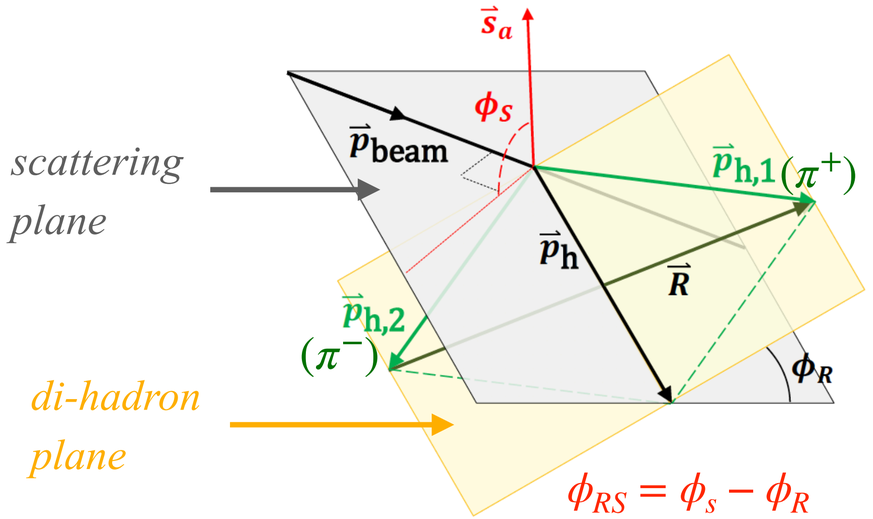

- **Cross-Ratio Method:**

$$A_{UT}sin(\phi_{RS}) = \frac{1}{P}\frac{\sqrt{N^{\uparrow}(\phi_{RS})N^{\downarrow}(\phi_{RS}+\pi)} - \sqrt{N^{\downarrow}(\phi_{RS})N^{\uparrow}(\phi_{RS}+\pi)}}{\sqrt{N^{\uparrow}(\phi_{RS})N^{\downarrow}(\phi_{RS}+\pi)} + \sqrt{N^{\downarrow}(\phi_{RS})N^{\uparrow}(\phi_{RS}+\pi)}}$$

$N^{\uparrow(\downarrow)} \rightarrow$ Number of $\pi^+\pi^-$ in respective ϕ_{RS} bin when the polarization is Up($\uparrow$) (Down ($\downarrow$)).
P is average beam polarization.

- Free from detector effects and associated uncertainties.

STAR Run 2015 Precision $A_{UT}^{\sin(\phi_{RS})}$ Measurement

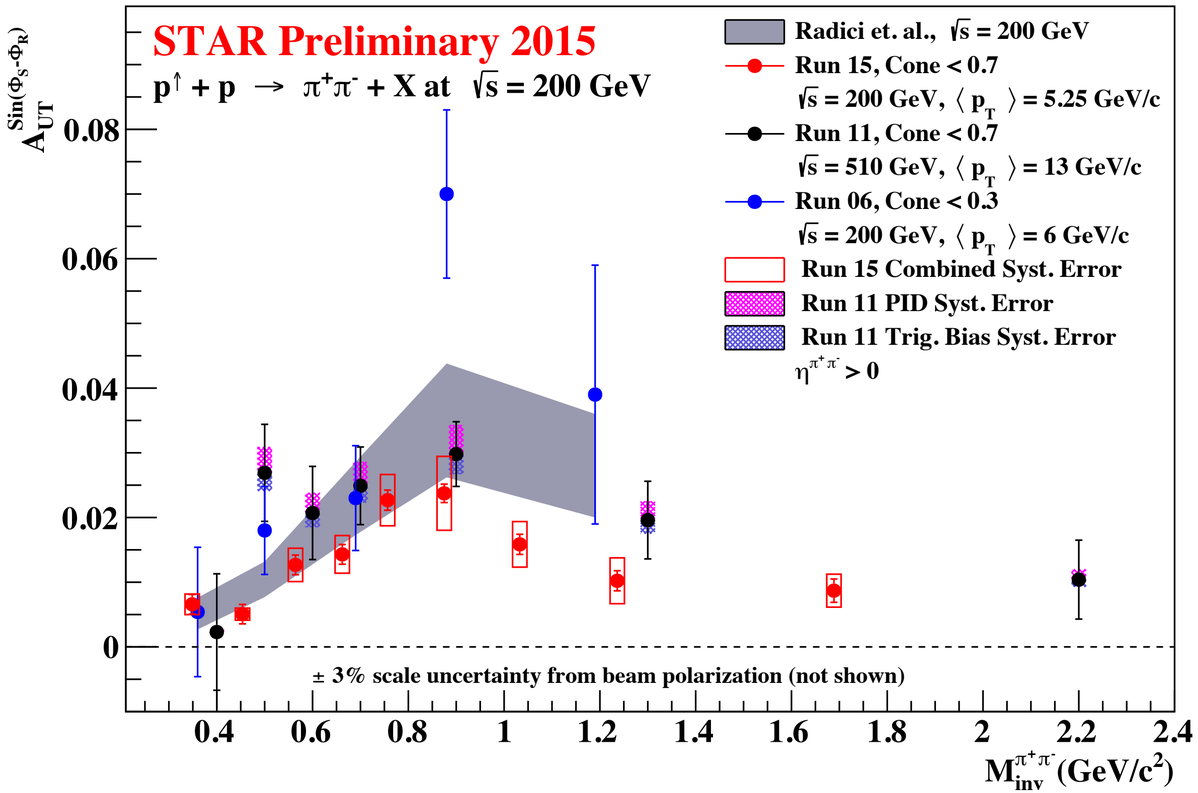

A_{UT} vs M_{inv}: A_{UT} is enhanced around $M_{inv}^{\pi^+\pi^-} \sim 0.8$, consistent with the previous measurement.

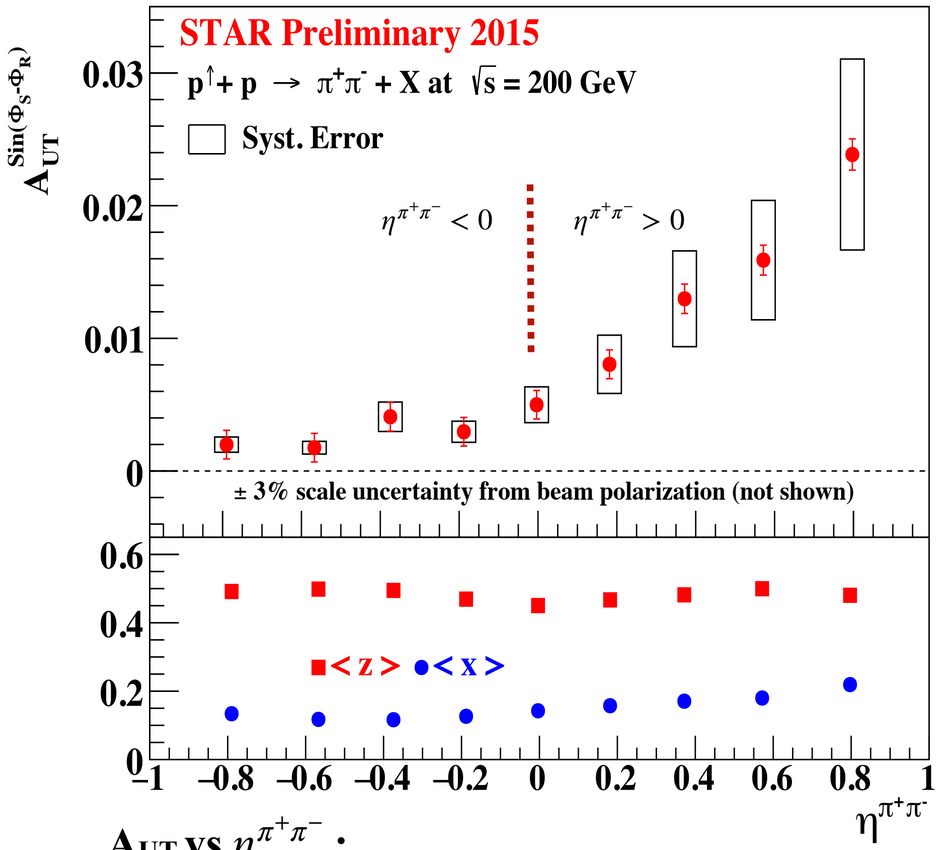

A_{UT} vs $\eta^{\pi^+\pi^-}$:

- Mean x and z as a function of $\eta^{\pi^+\pi^-}$ from simulation.
- $|\eta^{\pi^+\pi^-}| < 1$.
- **$0.1 < x < 0.22$, $z \sim 0.46$**

- **Significant A_{UT} in the forward region, where $h_1(x)$ is expected to be sizeable.**
- **Significant improvement in the statistical precision than previous STAR measurements.**

STAR Run 2015 Precision $A_{UT}^{\sin(\phi_{RS})}$ Measurement

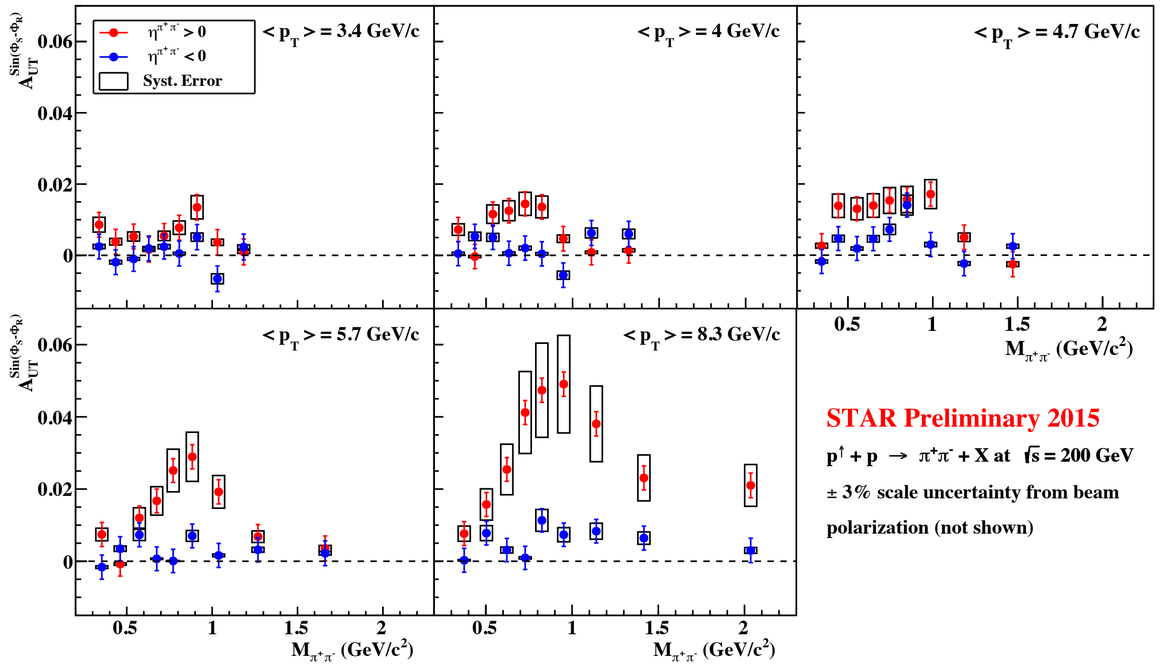

A_{UT} vs M_{inv} in $p_T^{\pi^+\pi^-}$ bins:

- 2D binning, A_{UT} as a function of M_{inv} in 5 p_T bins.
- Higher A_{UT} in the higher p_T bin, where higher x is probed.
- Growing prominence of the resonance peak around $M_{inv} \sim 0.8$ GeV/c^2 with increasing p_T.
- Small backward asymmetry, where lower x is probed.

- **Significant A_{UT} in the forward region, where $h_1(x)$ is expected to be sizeable.**
- **Significant improvement in the statistical precision than previous STAR measurements.**

STAR Run 2015 Precision $A_{UT}^{\sin(\phi_{RS})}$ Measurement

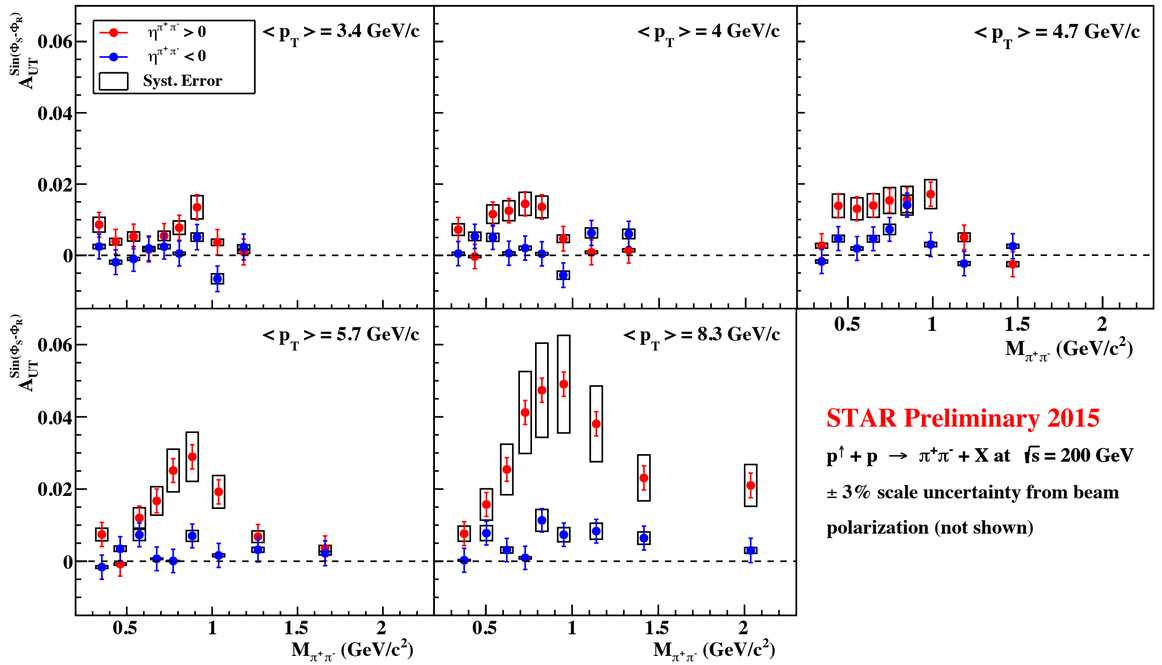

STAR Preliminary 2015

$p^\uparrow + p \rightarrow \pi^+\pi^- + X$ at $\sqrt{s} = 200$ GeV

± 3% scale uncertainty from beam polarization (not shown)

A_{UT} vs $p_T^{\pi^+\pi^-}$ in M_{inv} bins:

- 2D binning, A_{UT} as a function of $p_T^{\pi^+\pi^-}$ in 5 M_{inv} bins.
- A_{UT} increases with the p_T in the forward region, where higher x is probed.
- A_{UT} signal is larger when $M_{inv} \sim 0.8$ GeV/c^2 which is due to the resonance effect.
- Small backward asymmetry.

A_{UT} vs M_{inv} in $p_T^{\pi^+\pi^-}$ bins:

- 2D binning, A_{UT} as a function of M_{inv} in 5 p_T bins.
- Higher A_{UT} in the higher p_T bin, where higher x is probed.
- Growing prominence of the resonance peak around $M_{inv} \sim 0.8$ GeV/c^2 with increasing p_T.
- Small backward asymmetry, where lower x is probed.

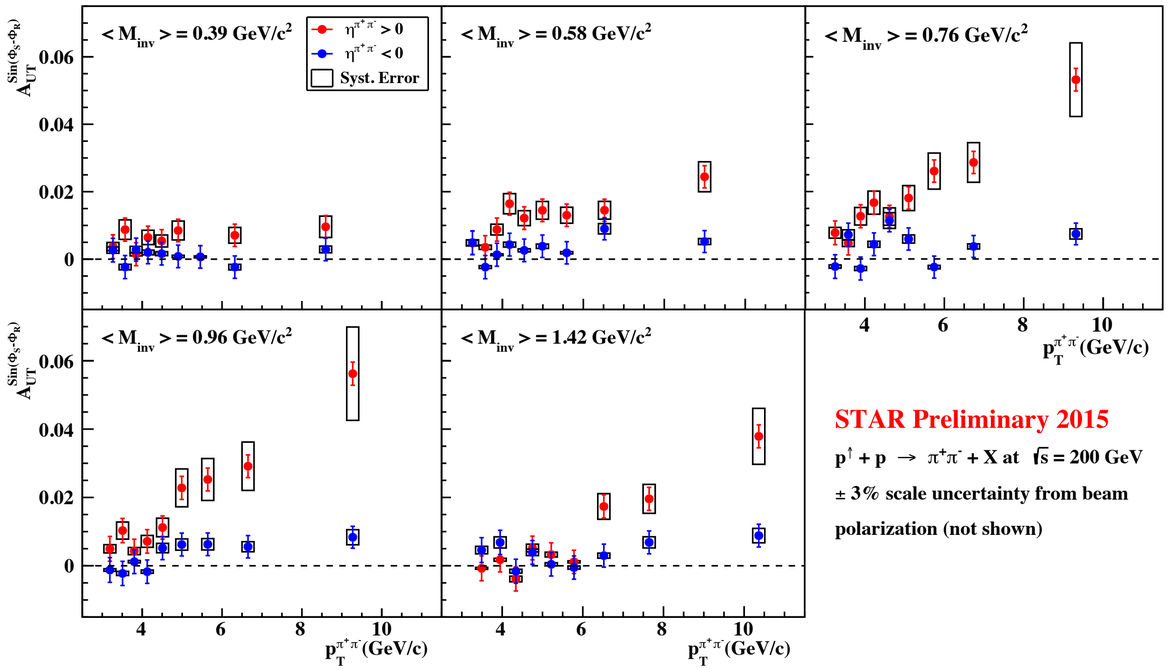

STAR Preliminary 2015

$p^\uparrow + p \rightarrow \pi^+\pi^- + X$ at $\sqrt{s} = 200$ GeV

± 3% scale uncertainty from beam polarization (not shown)

- **Significant A_{UT} in the forward region, where $h_1(x)$ is expected to be sizeable.**
- **Significant improvement in the statistical precision than previous STAR measurements.**

Unpolarized $\pi^+\pi^-$ Cross Section Measurement

$p + p \rightarrow \pi^+\pi^- + X$ at $\sqrt{s} = 200$ GeV from run 2012.

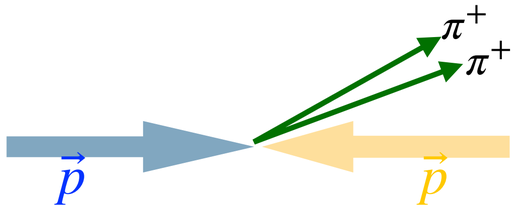

Polarization integrated ≈ Unpolarized

- Lower trigger threshold than 2015 dataset, and thus better for cross-section measurement.

- Inclusive $\pi^+\pi^-$ **differential cross section**:
  - As a **function of invariant mass, $M_{inv}^{\pi^+\pi^-}$, in $|\eta|<1$** .
  - Much needed for the $D_1^{h_1h_2}$ extraction.
  - Access to $D_1^{h_1h_2/g}$.

- We will release preliminary result very soon, STAY TUNED.

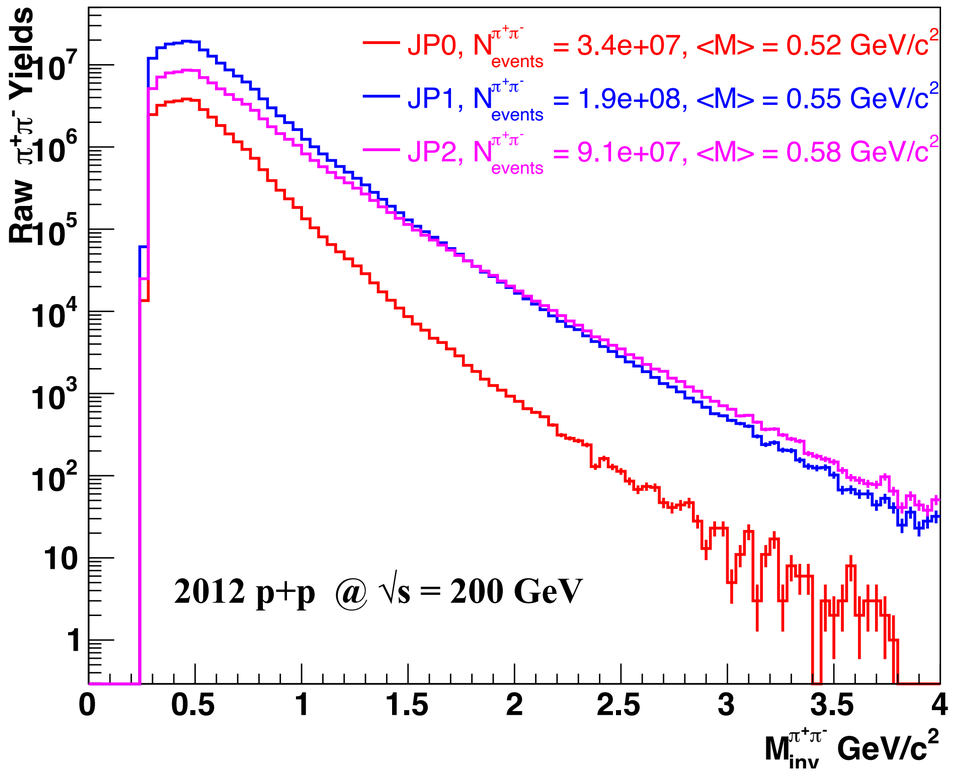

Summary

- **Azimuthal correlation asymmetries, which are sensitive to transversity, have been measured at STAR.**
  - The statistical precision of the new 2015 results is significantly improved compared to previous STAR measurements.
  - We expect to significantly reduce the systematic uncertainty from the PID by using the Time-of-Flight detector in the final result.

- **Preliminary result on the unpolarized dipion cross-section will be released VERY SOON using the STAR Run 12 data.**
  - Differential cross section as a function of $M_{inv}^{\pi^+\pi^-}$ in $|\eta|<1$.
  - Constrain unpolarized FF, D_1.

- **These measurements will provide a basis for the transversity extraction with better precision.**

- **These results can be used to test the universality between SIDIS, e^+e^-, and *pp* , and further constrain global fits of transversity, especially in the high *x* (0.1<*x*<0.3) region.**